Stochastic Approach to Rupture Probability of Short Fiber Reinforced Polypropylene for Automotive Crash Applications

N. Sygusch[1], N. Rüsch[2], B. Lauterbach[1], S. Kolling[3], J. Schneider[4]

[1]Crash Worthiness CAE, Adam Opel AG
[2]Institute of Plastics Engineering, Darmstadt University of Applied Sciences
[3]Institute of Mechanics and Materials, THM Gießen University of Applied Sciences
[4]Institute of Structural Mechanics and Design, Technical University Darmstadt

1 Introduction

Predicting rupture of short fiber reinforced plastics (SFRP) in numerical simulations can be a challenging task. Different mechanical properties, like e.g. anisotropy, strain rate dependency and brittle rupture behavior, need to be incorporated into the material model, in order to achieve reasonable results. In other studies, e.g. [2] and [4], the complete manufacturing process chain of SFRP was considered. In [6] and [7] the Tsai Hill criterion was used to study the rupture behavior of SFRP. However, the stochastic nature of the brittle rupture behavior has not been taken into consideration yet.
A simulation method for LS-DYNA® is proposed, where a rupture distribution function (RDF) instead of one particular rupture value is used, in order to include the material's experimentally determined rupture probability. One can directly incorporate the RDF into the simulation model, by using **`*DEFINE_STOCHASTIC_VARIATION`** in combination with certain material models, that allow these stochastic enhancements. The introduced method is applied on a polypropylene with 30 wt.% short glass fibers (PPGF30).

2 Methodology

A way of incorporating a distribution function in LS-DYNA® and combining it with certain material models is by using the keyword **`*DEFINE_STOCHASTIC_VARIATION`**. One can choose between cumulative and probability distribution functions. These can either be parameterized or defined by a load curve. Each integration point x_g of the finite element (FE) model is then assigned random scale factors R_S and R_F in order to scale either the materials' yield stress or the rupture strain [5].

$$\begin{aligned} \sigma_y &= R_S(x_g)\sigma_y(\varepsilon_{pl},...) \\ \varepsilon_{pl}^F &= R_F(x_g)\varepsilon_{pl}^F(\dot{\varepsilon},\varepsilon_{pl},...) \end{aligned} \tag{1}$$

One can use both techniques in combination running either coupled or uncoupled simulations or one can choose to use either one of them solely. Currently available material models are listed in Table 1.

Material number	Material model name
10	**`*MAT_ELASTIC_PLASTIC_HYDRO_STOCHASTIC`**
15	**`*MAT_JOHNSON_COOK_STOCHASTIC`**
24	**`*MAT_PIECEWISE_LINEAR_PLASTICITY_STOCHASTIC`**
81	**`*MAT_PLASTICITY_WITH_DAMAGE_STOCHASTIC`**
98	**`*MAT_SIMPLIFIED_JOHNSON_COOK_STOCHASTIC`**
123 (shells only)	**`*MAT_MODIFIED_PIECEWISE_LINEAR_PLASTICITY_STOCHASTIC`**

Table 1: Currently available material models for stochastical simulations (from [5])

The underlying concept of the stochastical simulation method is shown in Fig. 1. On the one side there is the mechanical testing, with consideration of e.g. anisotropy and strain rate dependency. The rupture behavior is statistically investigated by fitting a distribution function (e.g. a Normal or Weibull distribution). Depending on the used test method or the investigated material, the rupture behavior of force, displacement, stress or strain curves can be analyzed statistically. Performing goodness of fit tests, like the Kolmogorov-Smirnov (KS) or Anderson-Darling (AD) test, determine the quality of the resulting RDF fit. The numerical studies involve the parameter identification of the material model for the elastic constants and hardening curves. The resulting material card is then combined with a RDF into one single material card in order to model the stochastically distributed rupture behavior. For calibrating the material card one compares the rupture results of the simulations with the experimentally determined rupture distributions by means of Monte-Carlo-Simulation (MCS).

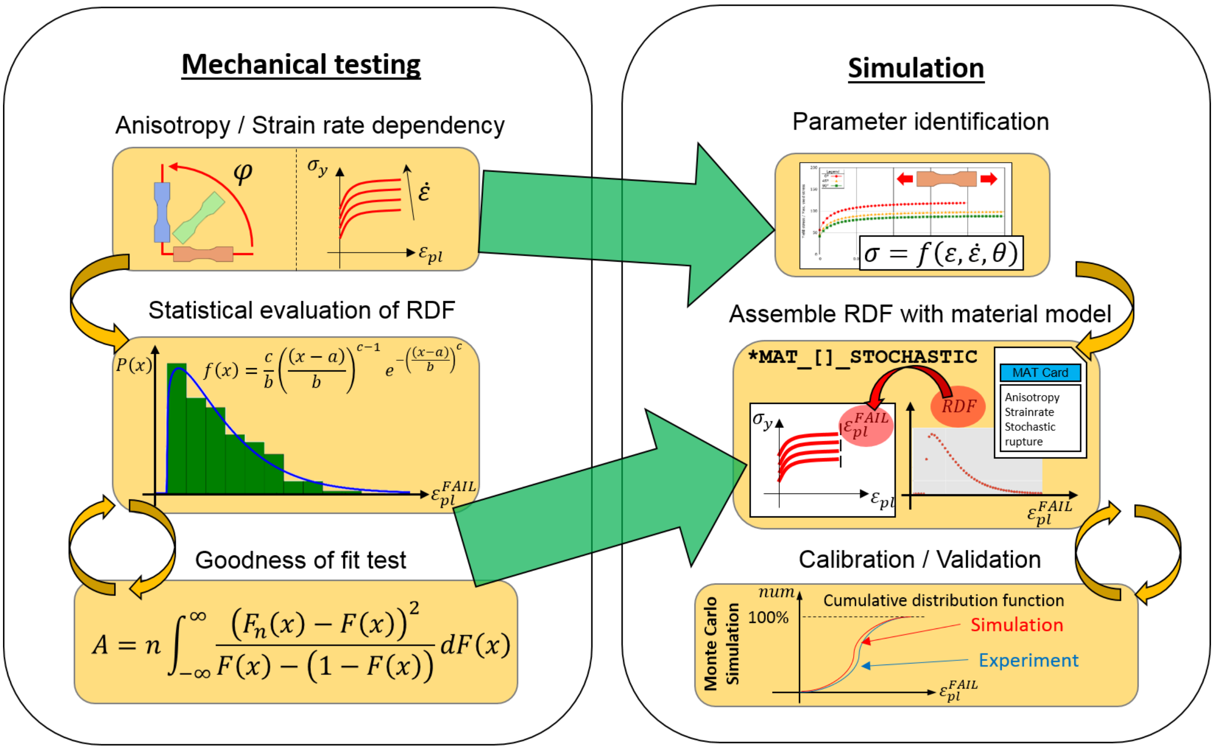

Fig.1: Flowchart stochastical simulation method

3 Experiments

The investigated material is a PPGF30. A number of at least 30 samples lay the foundations for the experimental studies. In order to take account for the anisotropy, four material directions, 0°, 30°, 45° and 90°, are considered during testing. The testing plan for the statistical quasi-static and dynamic three point bending tests is listed in Table 2. Fin and support radii are set to 2 mm.

Velocity	Nom. strain rate	Support	Orientation	Samples
0.001 m/s	0.021 /s	30 mm	0°, 30°, 45°, 90°	30 (50)
4 m/s	85 /s	30 mm	0°, 30°, 45°, 90°	30

Table 2: Statistical testing plan (specimen dimensions: 40x10x3.2 mm³)

The resulting mean values and confidence intervals for the maximum deflection and force levels are shown in Fig. 2. One can see that the maximum deflection ascends for the quasi-static tests, with increasing orientation angle, while the force level descends, which is typical for anisotropic materials like SFRP. For the dynamic tests however, the maximum deflection level does not ascend continuously with increasing orientation angle. It can be observed, that for the 90° orientation, the maximum deflection is below the level of the 0° orientation tests. A circumstance, which is strongly affiliated with the specimen’s microstructure on the one hand, and the increased impact velocity on the other hand [8].

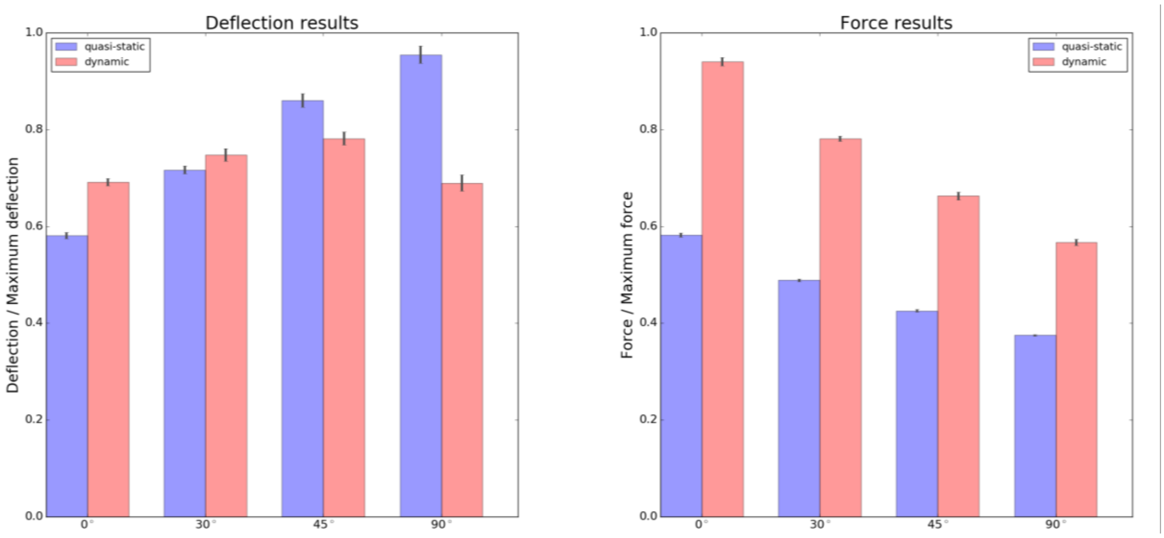

Fig.2: Results of maximum deflection and maximum force levels

Four distribution functions, namely the Normal and Log-normal distributions and the two and three parameter Weibull distributions, are studied and checked against the AD goodness of fit test.

$$AD = -n - \frac{1}{n}\sum_{i=1}^{n}(2i-1)\left(\ln\Psi(Z_i) + \ln\left(1-\Psi(Z_{n+1-i})\right)\right) \qquad (2)$$

In Eqn. (2) n is the number of samples and Ψ is the cumulative distribution function (CDF), with data $\{Z_i, \ldots, Z_n\}$.

The materials' best fit RDF for maximum deflections can be seen in Fig. 3. While the different distributions are easily distinguishable for the quasi-static tests, they mostly overlap for the dynamic tests. This is due to the fact of the materials' strain rate dependency, that with increasing orientation angle, the mechanical properties of SFRP accumulatively depend on the matrix material. For the quasi-static tests, the polypropylene matrix, shows progressive plastic yielding with increasing orientation angle. For the dynamic tests, on the other hand, the matrix shows brittle rupture behavior, and thus the mean of the maximum deflection levels of the different orientation angles are located closer to each other. Also notably is the changing order of maximum probability peaks of the 30° and 45° curves from the quasi-static to dynamic test velocity.

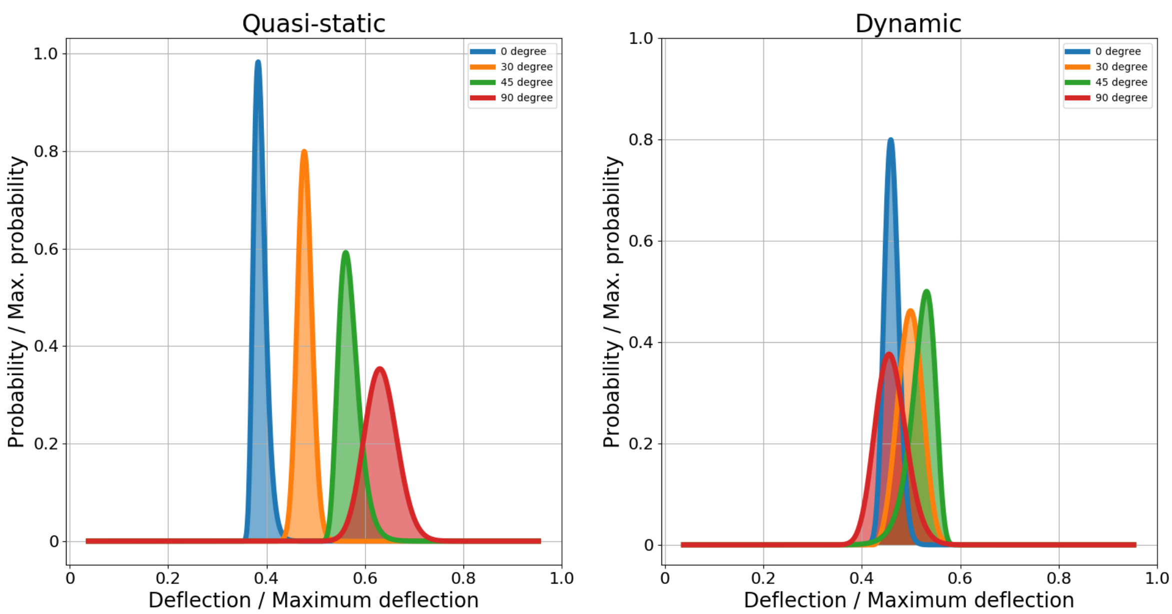

Fig.3: Statistical evaluation for maximum deflection

The resulting p-values of the AD test for the maximum deflections are listed in Table 3. For a given significance niveau of $\alpha = 5\%$ and test number of $n = 30$ the critical value for the AD statistic is 0.741 according to [1]. If a p-value for a probability function is below that critical value the null hypothesis for that probability function can be accepted, while it is rejected if the value is above 0.741. In this study the probability function with the lowest p-value is defined to most likely represent the distribution of the data and is therefore highlighted green in the table.

Velocity	Orientation	Normal	Log-normal	Weibull 3P	Weibull 2P
quasi-static	0°	0.404	0.228	0.248	0.976
	30°	0.537	0.530	0.573	0.987
	45°	0.451	0.340	0.415	0.965
	90°	0.300	0.266	0.281	0.781
dynamic	0°	0.429	0.395	0.470	1.015
	30°	0.227	0.237	0.208	0.268
	45°	0.843	0.854	0.463	0.404
	90°	0.317	0.259	0.264	0.630

Table 3: Goodness of fit tests (p-values) for maximum deflection

Though the differences between the resulting p-values may not be significant in some cases (e.g. dynamic 30°), it can be observed, that the Log-normal distribution gives the best results for 75% of the data. The three parameter Weibull distribution fits best for the dynamic 30° tests while the two parameter Weibull distribution fits best for the dynamic 45° orientation.

The best fit RDF for the maximum force levels are shown in Fig. 4. Except for fractional overlaps at the dynamic velocities all curves are arranged separately from each other. One can also observe, that the scatter is generally larger at the dynamic velocities, than at the quasi-static tests. It is noteworthy, that the 0° force curve of the quasi-static tests shows the largest scatter of all four orientations which is contrary to the deflection results, where the 0° curve showed the least scatter of all curves. This implies that both observations rely on separate mechanisms like fiber respectively matrix rupture. Also remarkable is, that the dynamic 30° curve shows the least scatter and highest peak of all four orientations, which indicates a better repeatability than the other orientations.

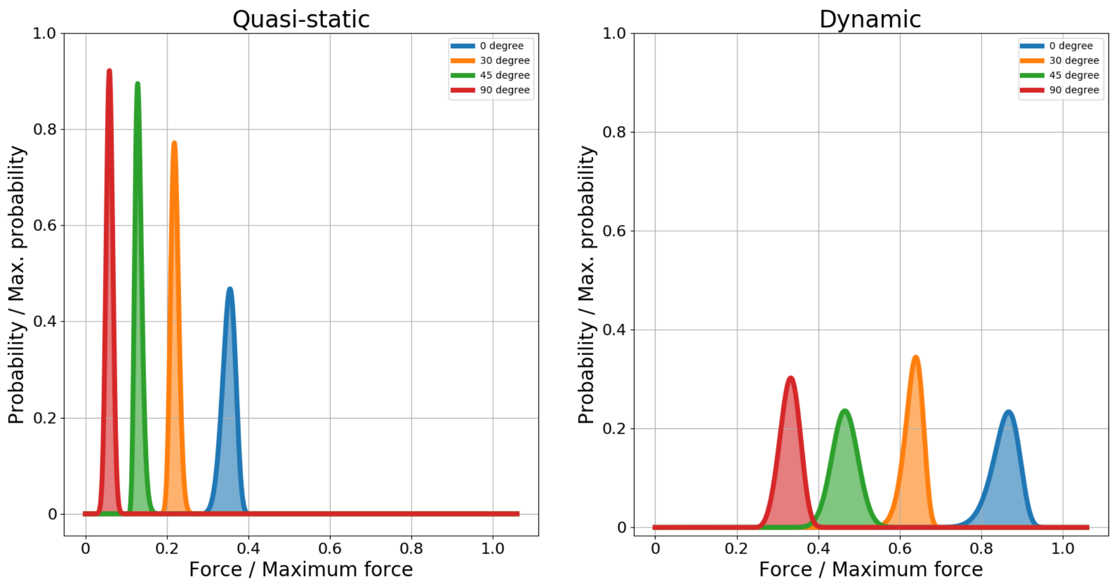

Fig.4: Statistical evaluation for maximum force

The resulting goodness of fit test values are listed in Table 4. The critical value remains the same, 0.741. The lowest values, in other words, the best fits, are highlighted in green again. Like before, the differences between certain distribution functions are not significantly large, e.g. at the 0° quasi-static curves. However, 75% of the quasi-static data appears to be Log-normal distributed, while 75% of the dynamic data turns out to be three parameter Weibull distributed.

Velocity	Orientation	Normal	Log-normal	Weibull 3P	Weibull 2P
quasi-static	0°	0.295	0.297	0.261	0.308
	30°	0.535	0.419	0.485	1.021
	45°	0.457	0.254	0.391	1.545
	90°	0.237	0.231	0.236	0.702
dynamic	0°	0.417	0.424	0.313	0.382
	30°	0.325	0.335	0.201	0.218
	45°	0.260	0.261	0.327	0.556
	90°	0.295	0.297	0.285	0.373

Table 4: Goodness of fit tests (p-values) for maximum force

4 Numerical simulations

The material model ***MAT_MODIFIED_PIECEWISE_LINEAR_PLASTICITY** (***MAT_123**) is used in this study. It's an elasto viscoplastic material model, similar to ***MAT_024** but has the advantage of enhanced rupture modelling capabilities. In order to investigate the properties of each orientation separately, one material card for every orientation is built. All simulations are run with fully integrated shell elements and nine integration points over the thickness, so the rupture behavior of the three point bending tests can be modeled appropriately. The numerical simulations listed below are carried out for the quasi-static tests, to investigate the stochastic parameters without the influences of dynamic effects.

4.1 Material characterization and calibration of friction

The elastic material constants and the parameters for the strain rate dependent hardening curves are identified by a reverse engineering optimization process via LS-Opt®. Further details on this process can be found in e.g. [3].
One decisive point in simulations involving contacts between multiple parts is the calibration of the friction parameter, since it can significantly influence the outcome of the simulation. As the three point bending test is no exception here, digital image correlation (DIC) can be a useful tool, in order to compare simulation and experiment. By measuring the length difference of two points on the specimens' surface over time and comparing it with the change of distance with equivalent node points in the simulation model one can use this information to appropriately calibrate the friction parameter (see Fig. 5).

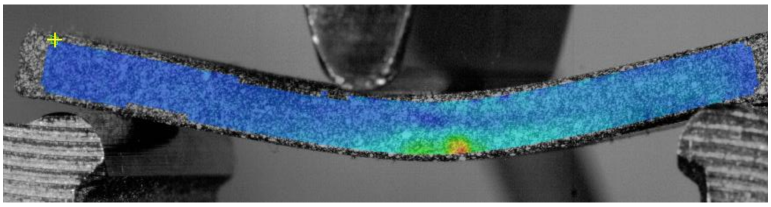

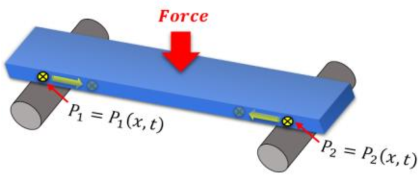

Fig.5: Using DIC with three point bending tests

Only one friction parameter for all orientations is set up. The material cards' parameters are adjusted simultaneously to fit the materials' global and local force deflection responses at the same time. The resulting curves for each orientation can be seen in Fig. 6.

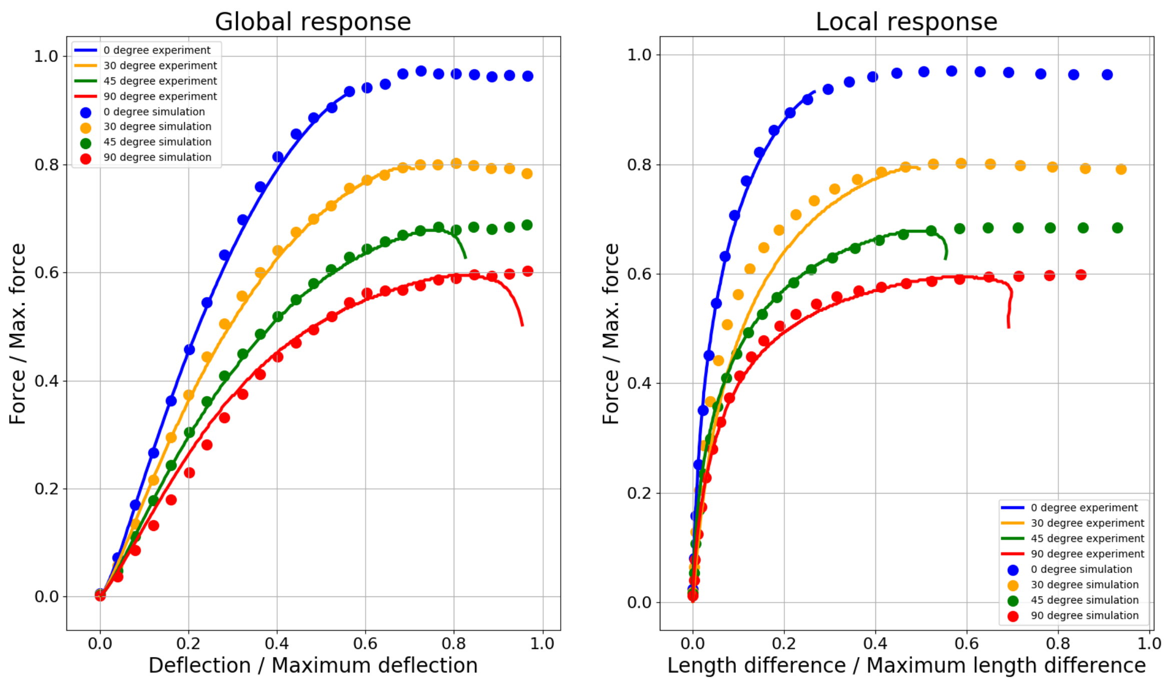

Fig.6: Global and local response correlations from three point bending tests

The intent is to fully calibrate the plasticity and friction of the model first before considering rupture. So at this stage, rupture has not been taken into account. For the onset as well as for the peak forces, the global force deflection results are in good agreement with the experiments. Since softening or damage are not considered at this point, the declining slope at the end of the 45° and 90° curves cannot be modelled sufficiently. The simulations of the local responses are also in good correlation with the experiments. Solely the onset of the 30° orientation could only be fitted to a certain degree. The peak force from the 30° orientation however, could be modelled accurately.

4.2 Calibration of rupture parameters

The material model **`*MAT_123`** offers three different kinds of rupture criteria:

- plastic strain to rupture
- thinning strain at rupture
- major in plane strain to rupture

In this study the rupture is investigated with help of the major in plane strain criterion. The calibration of the criterion is performed with an element size of 0.5 mm with nine integration points over the thickness. As the characteristic element length of full car simulations is usually larger than 0.5 mm a mesh study is performed to check for convergence of the calibrated rupture criterion. Mesh densities of 0.5 mm, 1.0 mm and 2.0 mm are tested. The results of the mesh study can be seen in Fig. 7.
The results from the 0.5 mm and 1.0 mm simulations show, that the discrepancy of both is not significantly large and the predicted rupture occurrence can be modelled accurately. For the 2.0 mm elements one can observe a step type rupture behavior in the simulations, which comes from the sequentially rupture of elements. With increasing characteristic element lengths however the gap between experimental rupture and simulation rupture increases. This effect can be incorporated with help of a regularization curve in future works.

For the 0° orientation the mechanical behavior is strongly dominated by the incorporated glass fibers which inherently show brittle rupture behavior. With increasing orientation angles, the matrix material progressively influences the mechanical behavior to a certain proportion. As the matrix material tends to mechanically behaves more ductile the observed deformations become larger.

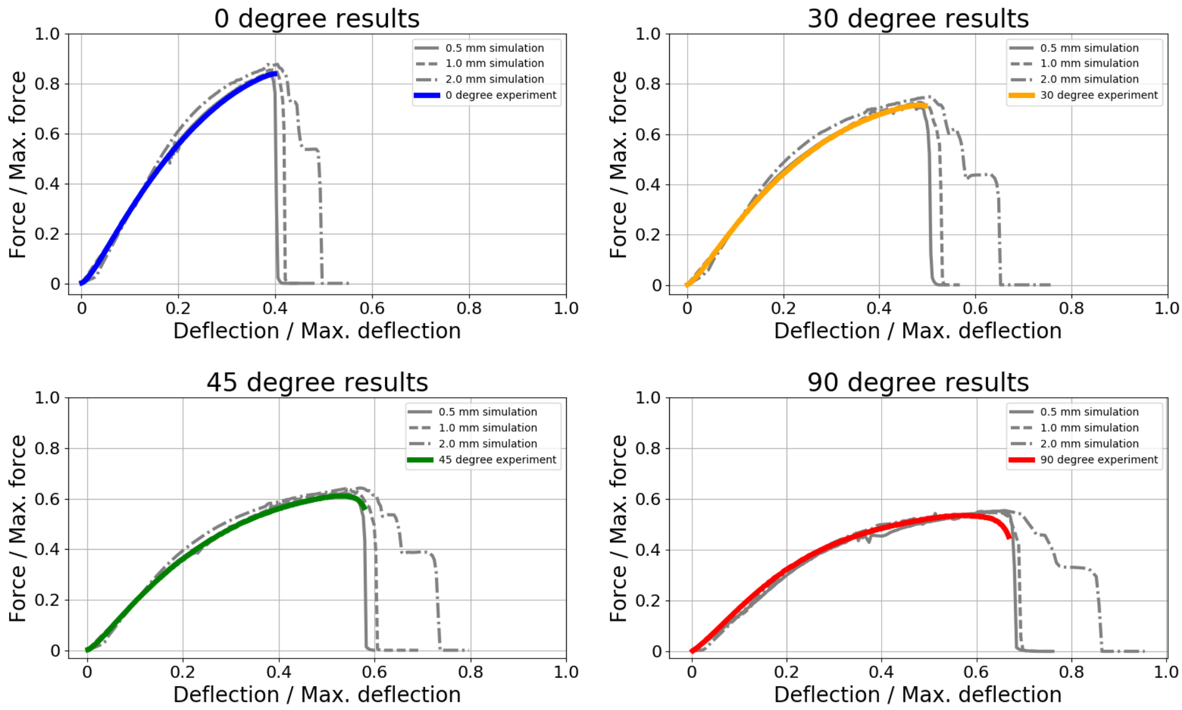

Fig.7: Mesh dependency study of the rupture criterion for all four orientations

4.3 Stochastic rupture modeling

In the previous studies one discrete rupture value is utilized in order to model the rupture behavior. To go beyond the concept of one particular value now, a continuous distribution function is used instead. The underlying idea is related to MCS, where N random variable experiments (simulations) are run and evaluated via statistical methods. The random variables are the major in plane strain rupture values in this case. The random variables can be assigned either to each element or each integration point. By using ***MAT_123_STOCHASTIC** one can make use of the latter method. One can then construct a normally distributed RDF (or any other RDF) with mean μ and standard deviation σ as a ***DEFINE_CURVE**, from which the solver picks random variables and assigns each integration point one discrete value.

The other option is to assign each element one specific rupture value. This can be done with help of an algorithm that searches for all elements and changes the properties in such a way, that each element has its own **PID** and a unique ***MAT_123** with a random variable from the RDF as input for the rupture value. An example for the resulting FE model can be seen in Fig. 8. The different colors of the elements are indicating different properties, like a unique **PID** and ***MAT_123**. To prevent redundancy in the stochastic simulations, the rupture value assignment for each element is completely randomized for each of the N runs.

For the stochastic simulations, a total number of 100 simulations are carried out. Fig. 9 generically shows the results for the 0° orientation. Two models, A and B, with different input parameters, are run and compared to each other in order to study the fundamental mechanics of the stochastic method. On the right side of Fig. 9 the input curves for the MCS are shown. The input curves for the major in plane strain distribution functions for model A and B are both Normal distribution functions. The Normal distribution functions of model A and B have the same mean values but the standard deviation of model A is greater than of model B, so in other words, the scatter of the input curve for model A is larger than for model B. The stochastic method is set up to assign each shell element of the specimen a random value from the given distribution function (see Fig. 8). One can then study the effects of different input curves on the outcome of the simulations.

The results for the 100 simulations are evaluated statistically. Note, that the input for both models is done via a strain Normal distribution function where the output is based on deflection distribution functions. Since force-deflection curves were measured during the three point bending experiments only these curves are of interest for this study. On the left side of Fig. 9 the evaluated distribution functions are shown. The evaluation of the simulations is done in the same manner as for the experiments. The resulting deflection distribution functions from the simulations are tested against the AD test in order to check the goodness of fit.
For model A the best fit distribution function for the resulting deflections shows a 3P Weibull distributed rupture behavior. For model B the resulting distribution function is a Normal distribution. From these observations it cannot be assumed that the class of distribution function which is given as input for the MCS naturally results when studying the output of the MCS. This point has to be further clarified in future studies. It can also be observed, that the scatter of the resulting distribution function of model A is significantly larger than for model B. So the greater input value of the standard deviation directly correlates to the outcome of the MCS. Noteworthy is, that the larger scatter of model A also results in a shift of the peak value from the curve. While the center of the strain distribution functions of both input curves were equal (right picture of Fig. 9), the resulting deflection distribution functions show an offset now (left picture of Fig. 9). Further studies have to clarify the influence and sensitivity of mean and standard deviation of the input curves on the results.
In a next step the resulting distribution functions from the MCS will also be compared to the experimental results. In addition, the resulting simulation curves could be further optimized by an algorithm that minimizes the differences between simulations and experiments.

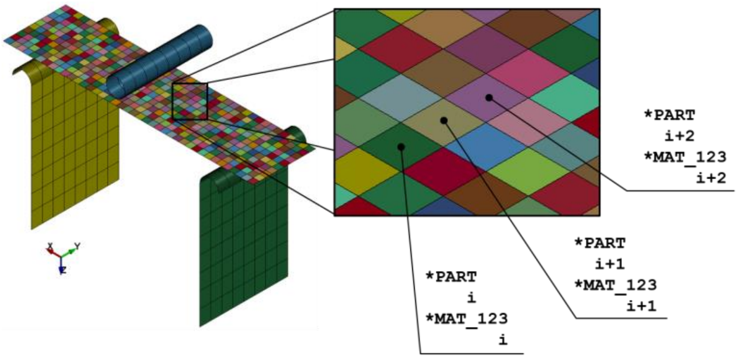

Fig.8: Finite element model for stochastic simulations (each ****MAT_123*** *has a different major in plane strain (**EPSMAJ**) rupture value)*

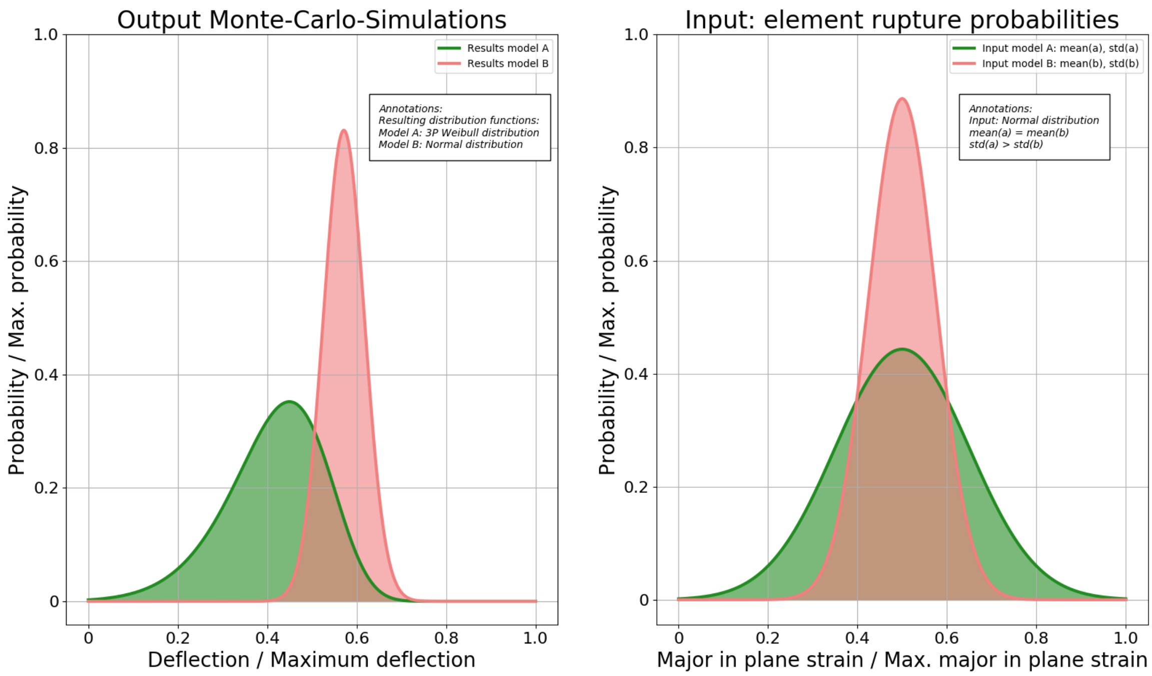

Fig.9: Input and output from the stochastic simulations for the 0° orientation

5 Summary

The presented study investigates the rupture of SFRP from a stochastic point of view. In the experimental part of this study, the maximum forces and deflections from quasi-static and dynamic three point bending tests are evaluated statistically. To ensure reliable conclusions from the experiments a minimum of 30 samples per orientation (0°, 30°, 45° and 90°) are performed. One essential observation from the experiments is, that the differences of the deflection levels in quasi-static testing velocities, for varying orientations, are significant, while they are vanishing for dynamic testing velocities.

Furthermore, simulations were performed to investigate the feasibility of modelling the observed stochastically phenomena numerically. In a first step the material is characterized with help of DIC to calibrate the non-linear mechanical behavior as well as the friction parameter. In a second step stochastical simulations are performed. Major in plane strain rupture distribution functions served as input curves for the Monte-Carlo-Simulations. A total number of 100 simulations for each test setup is performed, where each element of the specimen is assigned a unique rupture value from the distribution curve. The resulting simulations were analyzed statistically and the obtained deflection distributions are compared to each other quantitatively. Further work has to be done in order to be able to qualitatively compare the simulated RDF with the experimental results. Similarly to the goodness of fit tests mentioned above, a feasible quality criterion could determine the goodness of the simulated RDF proportionally to the observed probability functions from the experiments.

After calibrating the stochastical rupture behavior on coupon level one can then advance to the component level. An application may then be the field of robustness studies where one can investigate the sensitivity of structures made out of SFRP based on stochastical validated material cards.

6 Acknowledgment

The authors gratefully thank LyondellBasell for supplying the material investigated in this work.

7 Literature

[1] Dodson, B.: The Weibull Analysis Handbook, Milwaukee, Wis. ASQ Quality Press, Milwaukee, 2006

[2] Hatt, A.: Anisotropic modeling of short fibers reinforced thermoplastics materials with LS-DYNA, 13th German LS-DYNA Forum, Bamberg, 2014

[3] Haufe, A., Effinger, V., Reithofer, P., Rollant, M., Fritz, M.: Validation and Material Modelling of Plastics, 8th LS-DYNA European Users Conference, Strasbourg, 2011

[4] Lauterbach, B., Erzgräber, M., Liebold, C., Helbig, M., Haufe, A.: Closed Simulation Process Chain for Short Fiber Reinforced Plastic Components with LS-DYNA, 14th German LS-DYNA Forum, Bamberg, 2016

[5] N. N.: LS-DYNA® Keyword User’s Manual Volume I, Livermore Software Technology Corporation (LSTC), 2016

[6] Nutini, M., Vitali, M., Simulating anisotropy with LS-DYNA in glass-reinforced, polypropylene-based components. 9th German LS-DYNA Forum, Bamberg, 2010

[7] Nutini, M., Vitali, M., Erzgräber, M., Lauterbach, B.: Interactive Fracture Criterion for SGF-PP: Validation on Lower Bumper Support, 14th German LS-DYNA Forum, Bamberg, 2016

[8] Rüsch, N.: Experimentelle Untersuchung zur Wahrscheinlichkeitsverteilung des Versagens von kurzfaserverstärktem Polypropylen, Master Thesis, Darmstadt, 2016